Eur. Phys. J. Appl. Phys. **87**, 10302 (2019)

https://doi.org/10.1051/epjap/2019190007

THE EUROPEAN PHYSICAL JOURNAL APPLIED PHYSICS

Regular Article

Some physical properties of a $Li_4Ti_5O_{12}$ thin film electrode manufactured by radio frequency magnetron sputtering

Volkan Şenay[1,*] and Soner Özen[2]

[1] Department of Opticianry, Bayburt University, 69000, Bayburt, Turkey
[2] Department of Occupational Health and Safety, Yozgat Bozok University, 66300, Yozgat, Turkey

Received: 10 January 2019 / Received in final form: 16 July 2019 / Accepted: 31 July 2019

Abstract. A $Li_4Ti_5O_{12}$ thin film was fabricated on an ITO layer previously prepared on a glass microscope slide via RF magnetron sputtering technique. The structural, morphological, optical and electrochemical properties of the produced thin film were studied by several techniques. According to the findings, the investigated film has a crystalline structure with small grains. Its surface is nano-structured, dense and smooth. The system (LTO/ITO/glass) exhibits an average transmittance rate above 70% in the visible region with a band gap energy value of 3.8 eV. The obtained impedance spectrum shows a good blocking behavior. The Warburg diffusion element with a value of 817 $S.s^{1/2}$ provides easy Li-ion diffusion.

1 Introduction

Recently, all-solid-state rechargeable lithium-ion (Li-ion) micro-batteries have gained impetus due to the energy supply/storage necessity in various micro-system applications such as micro-sensors, micro-mechanics, micro-electronics, and the like [1–5]. Traditionally, micro-scale batteries consist of thin film ceramic materials as anode, electrolyte and cathode [1]. They are produced by sequential layer by layer deposition of the cell components using thin film manufacturing processes [1,5]. When compared to standard composite electrodes, thin-film electrodes exhibit significantly higher charge and discharge rates; therefore, they have the potential to increase the power density of thin film batteries [6]. By the way, various methods have been used for fabrication of thin film electrodes including chemical vapor deposition [7], RF magnetron sputtering [8], flash and thermal evaporation [9], pulsed laser ablation [10], spray coating [11], molten carbonate method [12] and sol–gel method [13].

Various kinds of Li-ion conductive materials and transition metal oxides have been proposed as electrolyte and electrode films for all-solid-state rechargeable Li-ion batteries [4,14]. Regarding the determination of safety and cycling life of Li-ion batteries, the anode materials often have a crucial role [15]. Carbon (graphite) is the anode material which is currently used in the majority of lithium-ion batteries. However, the carbon anode materials are facing safety issues caused by relatively low Li-intercalation potential (about 0 V vs. Li/Li^+) [16,17]. Since lithium titanate ($Li_4Ti_5O_{12}$, LTO) has a rapid Li^+ insertion and de-insertion ability, excellent cycle reversibility and high thermodynamic stability with its voltage plateau at 1.55 V versus Li/Li^+ and almost negligible volume change during the charge and discharge process [4,5,15–20], it can be considered as a promising alternative active material to replace graphite as the anode in rechargeable Li-ion batteries [15,19–21]. However, one disadvantage of LTO is its weak capacity at a high rate primarily due to its low electronic conductivity. LTO is an insulator with experimentally reported band gaps typically between 3.0 and 4.0 eV [22]. To overcome this drawback, many researchers have made enormous efforts to prepare nano-sized LTO [17,18]. When LTO nano-structures are synthesized, surface areas are increased and Li^+ diffusion lengths are decreased [22]. The aim of this study is to produce nano-scale LTO thin film anode material by RF magnetron sputtering method. RF magnetron sputtering has emerged as a useful method for producing high-quality thin films due to its repeatability, low cost, parameter controllability, high deposition rate and low processing temperature [23–25]. The optical, structural, morphological and electrochemical properties of the synthesized material were examined to find out its stability for developing rechargeable all-solid-state thin film Li-ion micro-batteries.

2 Experimental details

In the current research, a $Li_4Ti_5O_{12}$ thin film was sputtered onto a previously deposited ITO layer (on a glass microscope slide) by means of radio frequency (RF) magnetron sputtering technique with 75Watt (W) RF input power. The frequency of RF power was 13.56 MHz. A 99.5% purity $Li_4Ti_5O_{12}$ target having 50 mm diameter was used as source material. The substrate was placed on a substrate holder positioned at 40 mm away from the target. Argon (Ar) gas was used as buffer gas. The working pressure was approximately 6×10^{-2} Torr. The deposition

*e-mail: vsenay@bayburt.edu.tr

Table 1. Experimental parameters of the deposition process.

Substrate to target distance (mm)	Pressure (Torr)	RF Power (W)	Time (min)
40	6×10^{-2}	75	45

process was performed for 45 min under these conditions. The experimental parameters are summarized in Table 1. In order to prevent overheating, cooling water was used circulated through the chamber and sputter gun during the process.

The reflectance spectrum of the produced $Li_4Ti_5O_{12}$ thin film was obtained in the wavelength range of 400–1000 nm by a spectroscopic reflectometer (Filmetrics F20 Thin Film Analyzer). The surface morphology was examined by a field emission scanning electron microscope (FESEM) (Carl Zeiss SUPRA 40 VP). The normal incidence transmittance and absorbance data were collected by a UV-VIS double beam spectrophotometer (UNICO 4802) in the wavelength range of 300–1000 nm. A Tauc plot of $(\alpha h\nu)^2$ vs. $h\nu$ was used to estimate the optical band gap energy. X-ray diffraction measurement was carried out in the 2θ range of 20–70 by using an X-ray diffractometer (PANalytical Empyrean) with monochromated CuKα radiation ($\lambda = 1.54056$ Å) to examine the crystalline structure. Bragg-Brentano geometry and Pixel 3D detector were used for the XRD analysis. A potentiostat/galvanostat/ZRA device was used for electrochemical measurements (Gamry Reference 3000). The produced $Li_4Ti_5O_{12}$/ITO/glass system was immersed in the 0.1 M lithium perchlorate propylene carbonate ($LiClO_4$-PC) electrolyte. A standard three-electrode cell was adopted with $Li_4Ti_5O_{12}$/ITO/glass as the working electrode (WE), ITO/Glass as the counter electrode (CE) and Ag/AgCl as the reference electrode (RE). Cyclic voltammetric (CV) and impedance analysis were carried out with the scan rate of 1 mV/s.

3 Results and discussion

Figure 1a shows a top view FESEM image of the LTO thin film deposited on ITO/glass substrate. The surface of the obtained thin film is nano-structured, dense and smooth (having low roughness) without the presence of voids or pores. However, it can be observed from the figure that the film is not free from nano-cracks. The growth mode of the film was determined to be layer-plus-island mode (Stranski-Krastanov growth mode). Figure 1b shows the XRD pattern of the LTO thin film deposited on ITO/glass substrate. As shown in Figure 1b, LTO and ITO crystal phases were detected. No other diffraction peak was detected except ITO and LTO peaks. The crystal direction of the LTO was found to be (400), (331) and (531). The positions of the peaks are in good agreement with existing literature [26]. Other peaks correspond to the (211), (222), (332), (431) and (622) diffraction planes of ITO as reported in relevant literature [27,28]. The average crystallite size was calculated using the Debye-Scherrer's equation as follows:

$$D = \frac{k\lambda}{\beta \cos\theta} \tag{1}$$

where D is the crystallite size, λ is the X-ray wavelength, β is the full width at half maximum, θ is the Braggs diffraction angle and k is constant (0.94). The average crystallite size was calculated by resolving the highest intensity peak of LTO, i.e., (400) plane. The average crystallite size of the LTO thin film was found to be 22 nm which gives an indication that the produced LTO thin film has a nano-crystalline structure.

Figure 2a–c presents the optical transmittance (T), absorbance (A) and reflectance (R) spectra of the LTO thin film deposited on ITO/glass substrate. The T, A and R spectra of the uncoated glass, ITO/glass and LTO/glass are also given for better comparison in the figure. The T, A and R levels of ITO/glass and LTO/glass are quite identical. These systems have an average transmittance rate above 80% in the visible region from 400 to 700 nm. When LTO was deposited on ITO/glass, it was observed that the transmittance decreased and the absorbance and reflectance increased. However, the LTO/ITO/glass system exhibited an average transmittance rate above 70% in the visible region which is sufficient for practical applications. The oscillatory character of the transmittance and reflectance curves of LTO/ITO/glass is due to the interference effect arising from the multiple reflections at the interfaces which indicates the thickness uniformity of the film.

The optical band gap energy value of the LTO thin film deposited on ITO/glass substrate can be obtained by the well-known Tauc method [29]:

$$(\alpha h\nu)^2 = B(h\nu - E_g), \tag{2}$$

where α is the optical absorption coefficient, $h\nu$ is the energy of the incident photon, B is a constant and E_g is the optical band gap energy. The value of the exponent indicates the nature of the electronic transition, whether allowed or forbidden and whether direct or indirect: for direct allowed transitions: 2, for direct forbidden transitions: 2/3, for indirect allowed transitions: 1/2, for indirect forbidden transitions: 1/3. Plotting the $(\alpha h\nu)^n$ vs. $h\nu$ is a matter of testing $n = 1/2$ or $n = 2$ to compare which provides the better fit and thus identifies the correct transition type. $(\alpha h\nu)^2$ curve as a function of $h\nu$ was plotted to obtain the optical band gap energy value, as shown in Figure 2d. The single slope in the figure asserts that the produced systems have direct and allowed transition. The optical band gap energy value obtained by the Tauc method is 3.8 eV for the LTO thin film deposited on ITO/glass substrate. Such a band gap energy value is typical of electronically insulating materials and it is in good agreement with the relevant literature [30].

The impedance spectrum and Randles circuit obtained from the electrochemical impedance analysis are given in Figure 3. The Randles circuit showed that the anode electrode had a semi-infinite linear diffusion controlled faradaic reaction and the values for ionic transfer resistance (R_1), capacitance (Q), charge transfer resistance (R_2) and

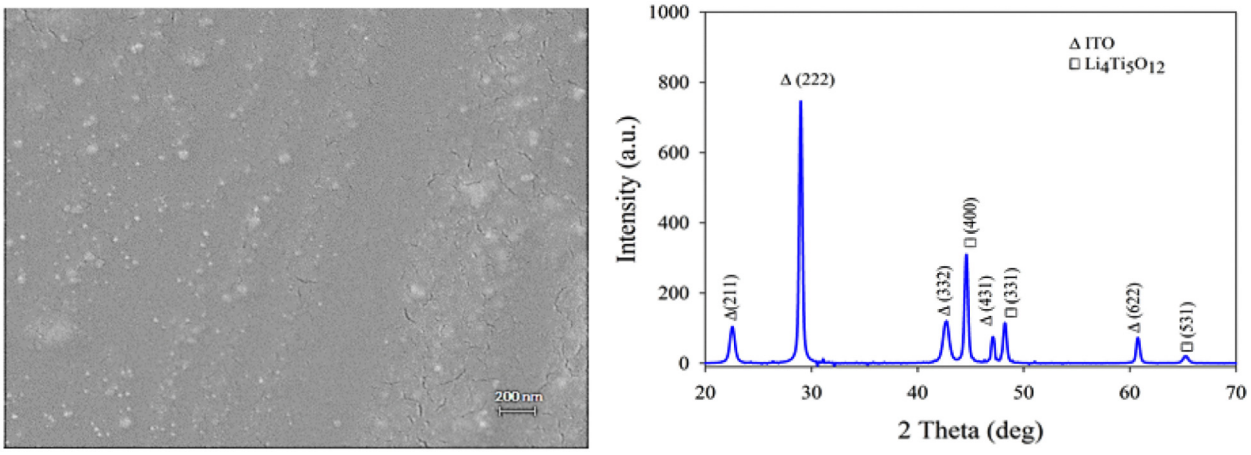

Fig. 1. (a) Top view FESEM image and (b) XRD pattern of the LTO thin film deposited on ITO/glass substrate.

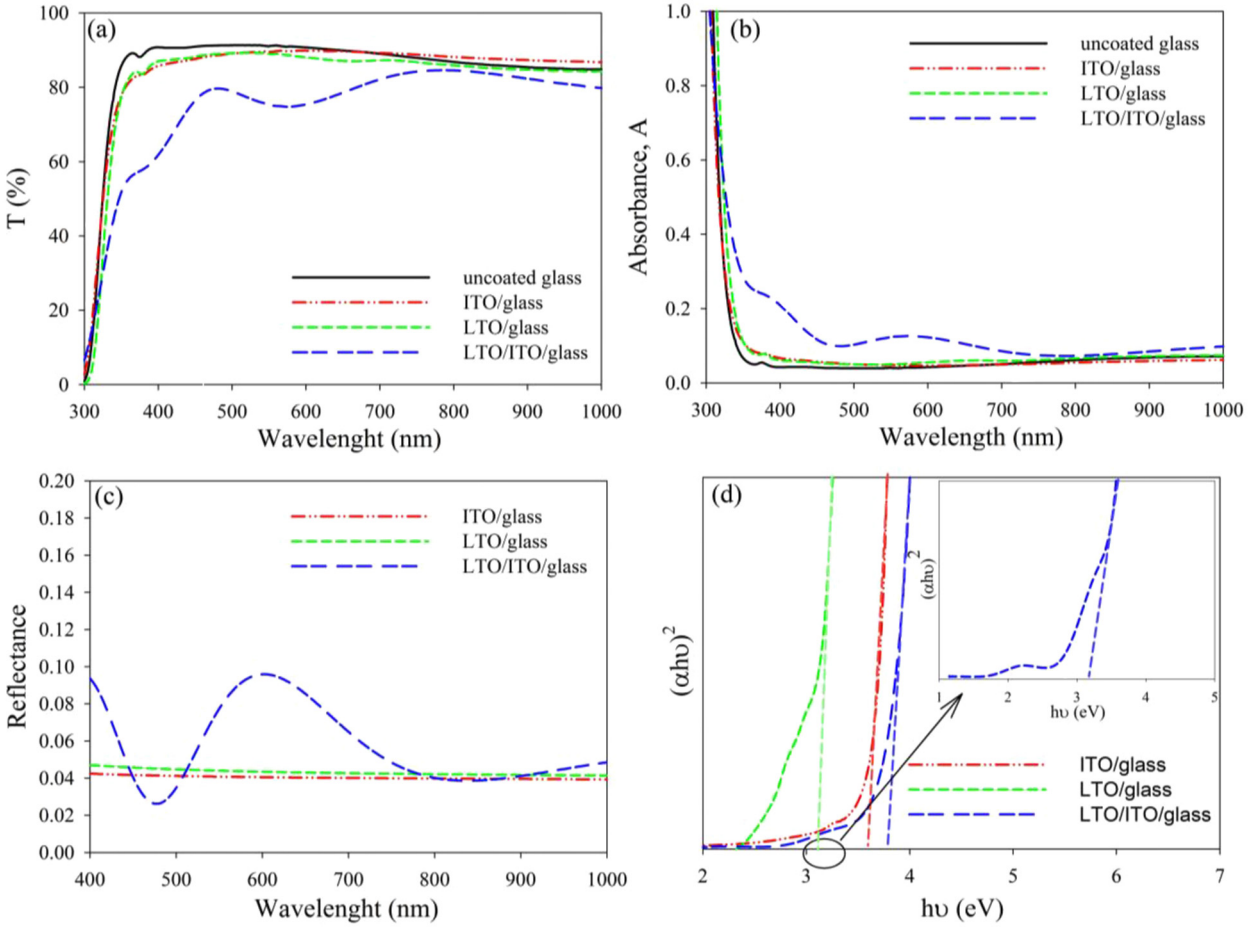

Fig. 2. (a) Transmittance, (b) absorbance, (c) reflectance spectra of the LTO thin film deposited on ITO/glass substrate and (d) Tauc plot of $(\alpha h\nu)^2$ vs. $h\nu$ to obtain the optical band gap energy.

Warburg impedance (Z_w) are given in Table 2. The ionic transfer resistance was determined as 527 Ω· The conductivity of the $LiClO_4$-PC electrolyte is approximately 2.0 mS. The ionic transfer conductivity value at the anode electrode-electrolyte interface was calculated as 1.9 mS from the relation $1/R_1$. This value is in good agreement with the conductivity value of $LiClO_4$-PC electrolyte. The impedance spectrum showed a good blocking behavior representing a capacitive branch in the tracking of a transmission line, i.e. the anode shows a high charge transfer resistance. This is due to repeated intercalation of lithium ions into the LTO anode. The constant phase capacitance of LTO anode material is 18 μF. The Warburg diffusion element with a value of 817 $S.s^{1/2}$ provides easy Li-ion diffusion. However, charge transfer is low owing to the charge transfer resistance of 600 kΩ. The produced

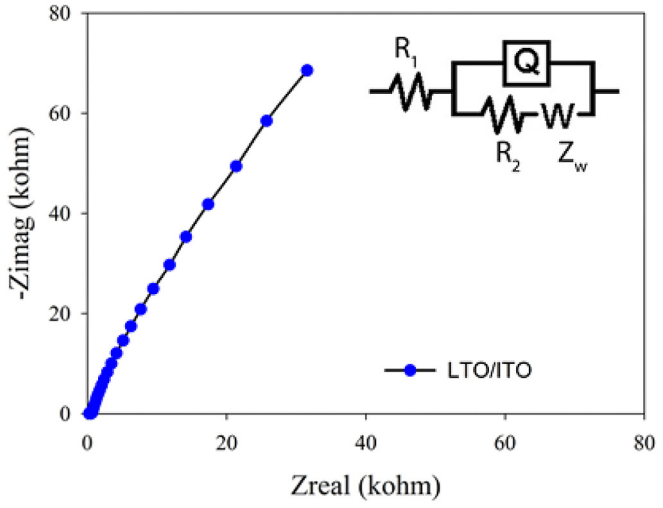

Fig. 3. The impedance spectrum and Randles circuit obtained from the impedance analysis.

Table 2. The obtained ionic transfer resistance (R_1), capacitance (Q), charge transfer resistance (R_2) and Warburg impedance (Z_w) values from the electrochemical impedance analysis.

R_1 (Ω)	Q (μF)	R_2 (kΩ)	Z_w (S.s$^{1/2}$)
527	18	600	817

LTO anode layer has better ionic conductivity when compared to related studies in literature [31–33].

4 Conclusions

In summary, RF magnetron sputtering deposition of LTO nano-particles was studied to prepare a thin film on transparent conducting oxide, namely ITO/glass substrate as anode for Li-ion micro-batteries. The produced thin film was not exposed to thermal treatment. FESEM analysis revealed that the surface of the thin film obtained by this process was dense and smooth. X-ray diffraction study confirmed that the crystallinity of the $Li_4Ti_5O_{12}$ was conserved in the deposited layer. Optical study revealed that LTO/ITO/glass exhibits an average transmittance rate above 70% in the visible region with a band gap energy value of 3.8 eV. The half-cell impedance performance of LTO anode was investigated. The obtained Randles circuit showed that the anode electrode had a semi-infinite linear diffusion controlled faradaic reaction. The impedance spectrum showed a good blocking behavior due to repeated intercalation of lithium ions into the LTO anode. Easy Li-ion diffusion was achieved; however, charge transfer was low. The originality of this study is the production of solid state LTO thin film anode with low current and high-performance properties providing corrosion resistance due to its high charge transfer resistance. In the light of the obtained results, although several deposition procedures have been reported for producing thin film $Li_4Ti_5O_{12}$ electrodes, RF magnetron sputtering comes out to be as a simple and cost-effective technique. This technique can be an alternative for preparing nano-structured $Li_4Ti_5O_{12}$ thin film anodes for Li-ion micro-batteries.

Author contribution statement

Volkan Şenay and Soner Özen contributed to the design and implementation of the research, to the analysis of the results and to the writing of the manuscript.

References

1. N.A. Kyeremateng, T.M. Dinh, D. Pech, RSC Adv. **5**, 61502 (2015)
2. J. Xie et al., Solid State İonics **287**, 83 (2016)
3. K. Tadanaga et al., J. Asian Ceramic Soc. **3**, 88 (2015)
4. Y.H. Rho, K. Kanamura, Hyomen Kagaku. **24**, 423 (2003)
5. J. Mosa et al., J. Power Sources **244**, 482 (2013)
6. M. Roeder et al., J. Power Sources **301**, 35 (2016)
7. S.-I. Cho, S.-G. Yoon, J. Electrochem. Soc. **149**, A1584 (2002)
8. B. Wang et al., J. Electrochem. Soc. **143**, 3203 (1996)
9. C. Julien et al., Appl. Surface Sci. **65**, 325 (1993)
10. K. Striebel et al., J. Electrochem. Soc. **146**, 4339 (1999)
11. T. Uchiyama et al., J. Electrochem. Soc. **147**, 2057 (2000)
12. I. Uchida, H. Sato, J. Electrochem. Soc. **142**, L139 (1995)
13. Y.H. Rho, K. Kanamura, T. Umegaki, J. Electrochem. Soc. **150**, A107 (2003)
14. Y.H. Rho et al., Solid State Ionics **151**, 151 (2002)
15. B.V. Babu et al., Results Phys. **9**, 284 (2018)
16. H. Deng et al., J. Nanomater. **2018**, 1 (2018)
17. Y.-R. Zhu et al., J. Chem. Sci. **126**, 17 (2014)
18. J. Zhang et al., J. Nanopart. Res. **15**, 2005 (2013)
19. X. Sun et al., Int. J. Electrochem. Sci. **9**, 1583 (2014)
20. F.K. Dokan et al., Acta Phys. Pol. A **125**, 648 (2014)
21. Z. Yu et al., Energy Technol. **2**, 767 (2014)
22. M.G. Verde et al., ACS Nano **10**, 4312 (2016)
23. A. Mantarci, M. Kundakçi, Bull. Mater. Sci. **42**, 196 (2019)
24. A. Mantarcı, M. Kundakçi, Opt. Quant. Electr. **51**, 81 (2019)
25. A. Mantarcı, M. Kundakçı, in *AIP Conference Proceedings* (AIP Publishing, 2017), p. 020119s
26. Z. Wang, G. Xie, L. Gao, J. Nanomater. **2012**, 9 (2012)
27. D. Choi, S.-J. Hong, Y. Son, Materials **7**, 7662 (2014)
28. H.H. Yudar et al., Appl. Phys. A **122**, 748 (2016)
29. J. Tauc, R. Grigorovici, A. Vancu, Phys. Status Solidi (b) **15**, 627 (1966)
30. C. Kim et al., Adv. Funct. Mater. **23**, 1214 (2013)
31. F. Wu et al., J. Alloys Compd. **509**, 596 (2011)
32. D. Wang et al., Ceram. Int. **40**, 3799 (2014)
33. Y. Sun et al., Electrochim. Acta **246**, 106 (2017)

Cite this article as: Volkan Şenay, Soner Özen, Some physical properties of a $Li_4Ti_5O_{12}$ thin film electrode manufactured by radio frequency magnetron sputtering, Eur. Phys. J. Appl. Phys. **87**, 10302 (2019)